European Journal of Pharmaceutical Sciences 121 (2018) 309–318

Contents lists available at ScienceDirect

European Journal of Pharmaceutical Sciences

journal homepage: www.elsevier.com/locate/ejps

Comparative behavior between sunscreens based on free or encapsulated UV filters in term of skin penetration, retention and photo-stability

Arianna C. Cozzi[a,b], Paola Perugini[a], Samuel Gourion-Arsiquaud[b,*]

[a] Department of Drug Science, University di Pavia, via Taramelli 11, Pavia, Italy
[b] TRI Princeton, 601 Prospect Ave, Princeton, NJ, USA

ARTICLE INFO

Keywords:
Encapsulated UV filter
Skin penetration
Avobenzone
FTIR imaging spectroscopy
Sunscreen efficacy evaluation

ABSTRACT

Background: The growing incidence of photodamaging effects caused by UV radiation (e.g. sunburn, skin cancer) has increased the attention from health authorities which recommend the topical application of sunscreens to prevent these skin damages. The economic stakes for those companies involved in this international market are to develop new UV filters and innovative technologies to provide the most efficient, flexible and robust sunscreen products. Today the development of innovative and competitive sunscreen products is a complex formulation challenge. Indeed, the current sunscreens must protect against skin damages, while also being safe for the skin and being sensory and visually pleasant for the customers when applied on the skin. Organic UV filters, while proposing great advantages, also present the risk to penetrate the stratum corneum and diffuse into underlying structures with unknown consequences; moreover, their photo-stability are noted thorny outcomes in sunscreen development and subsequent performance. In recent years, the evaluation of the interaction between skin and sunscreen in terms of penetration after topical application has been considered from European authority but still its testing as their photo-stability assessment are not mandatory in most countries.

Objective: This study, based on in-vitro approaches, was performed to evaluate and compare the retention and the penetration of organic UV filters in free or encapsulated form inside the skin as well as their respective photo-stability.

Methods: Sunscreen formulation with a combination of Avobenzone and Octocrylene in "free form" and a formulation using the same UV filters but encapsulated in a sol-gel silica capsule, were analyzed and compared by FTIR Imaging Spectroscopy. Tape stripping method was used to investigate the penetration of these UV filters inside the stratum corneum. Their photo-stabilities were evaluated by spectroscopic measurements (FTIR, UV/Vis) and standard measurements were calculated: AUC (Area Under the Curve) and SPF (Sun Protection Factor).

Result: With traditional formulation, the organic UV filters penetrated significantly into the stratum corneum while the same UV filters combined with encapsulation technology remained on the skin surface. The encapsulation technology also improved significantly their stability.

Conclusion: Encapsulation technology is a promising strategy to improve the efficacy of sunscreen product using organic UV filters and to reduce safety problem. On the other hand, this study highlighted the pertinence of the FTIR Spectroscopy to test, compare and investigate sunscreen formulations.

1. Introduction

UV radiations represents only 5–10% of solar radiations but constitute a major hazardous risk for human health with acute adverse outcomes like sunburns and chronic ones like skin cancer (IARC, 2012). Our first and main defense line against the UV radiation is our skin but this barrier does not provide a total protection and a significant part of these UV radiations penetrates our body. UVB penetrates the upper layers of the skin while UVA penetrates the deepest skin layer and interacts with DNA. When skin cell DNA absorbs UV radiation, cross-linking of pyrimidine bases can occur (Setlow, 1966); when damaged DNA dimers are not repaired, mutations are created and can ultimately lead to skin cancer (Holick, 2004; Halliday, 2014; Brash et al., 1991). To reduce the effects of overexposure to UV radiation the international health authorities have recommended the use of sunscreen products which are currently commonly apply all over the globe. To respond to this international market need, the companies develop new UV filters and innovative technologies to provide the most efficient and flexible

* Corresponding author.
E-mail address: sgourion@triprinceton.org (S. Gourion-Arsiquaud).

https://doi.org/10.1016/j.ejps.2018.06.001
Received 1 March 2018; Received in revised form 11 May 2018; Accepted 2 June 2018
Available online 03 June 2018

sunscreen products. The development of efficient and innovative sunscreens is a complex formulation challenge as more and more UV filters are incorporated into day-to-day products such as moisturizers, creams, lip sticks and other skin care products. The current sunscreens must protect against skin damages associated to sun exposure, while also being safe for the skin and being sensory and visually pleasant for the customers when applied on the skin.

UV filters are the key ingredients of sunscreen, providing the essential protection against skin photodamages. In order to guarantee skin protection, the ideal sunscreen product should create a stable protective film on the outermost layer of the skin to absorb or reflect the UV radiations (Jiang et al., 1997; Lu, 1999) during the entire period of UV exposure (Nash and Tanner, 2014). The reality is different especially for organic UV filters. While organic UV filters offer significant cosmetic advantages compared with inorganic UV filters (Mancebo et al., 2014), they have been challenged for their poor photostability (Afonso et al., 2014; Gonzenbach et al., 1992; Schwack and Rudolph, 1995) and for their safety (Gonzalez, 2010; Gonzalez et al., 2006). Indeed, the photo instability of these UV filters can lead to photochemical reactions which compromise both their physical (color, appearance) and chemical properties (efficacy). Chemical alterations can cause undesirable reactions as the production of inactive sunscreen products or highly reactive molecules that can react with the skin (Damiani et al., 2010; Vallejo et al., 2011). Regarding safety, some studies have shown that these organic UV filters could penetrate the stratum corneum SC (Hayden et al., 2005) and diffuse into underlying skin structures. Few studies highlighted their potential systemic absorption as they were detected in human plasma and urine (Janjua et al., 2008) and in 85% of Swiss human milk samples (Schlump et al., 2010). New formulations of organic UV filters-based sunscreens are necessary to reduce their skin penetration and diminish at once their toxicological risks and efficacy.

Avobenzone (Butyl Methoxydibenzoylmethane) is one of the most common organic UV filters for its strong UVA protection and its versatility (Shaath, 2010; Cabrera et al., 2014). However, it has been reported to have a significant photo instability (Afonso et al., 2014; Gonzenbach et al., 1992; Schwack and Rudolph, 1995) and to lead to photo-allergies (Schauder and Ippen, 1986; Motley and Reynolds, 1989). To increase avobenzone photo-stability and efficacy, it is typically combined with a variety of photo-stabilizers, including other UV filters such as octocrylene (Cantrell and JMcGarvey, 2001). Innovative technologies have also been developed to improve the efficacy and the safety of these actives. Encapsulation is becoming a technique widely explored by the pharmaceutical and chemical industries and its incorporation in cosmetics and personal care products has shown great expansion. Microencapsulation is a process of encapsulating an active ingredient into a shell permanently or temporarily. The result is capsules having diameter between 1 to few micrometers providing a large surface area that could be available for sites of adsorption and desorption, chemical reactions, light scattering, etc. (Benita, 2005; Jyothi et al., 2010; Kaur and Sharma, 2013). Using this technique, encapsulated UV filters, do not have direct contact with the skin which concomitantly prevents their potential toxicological risks.

In the present study, we investigated and compared the behavior of sunscreen formulations based on the same combination of organic UV Filters, Avobenzone and Octocrylene (Eusolex OCR), in free or encapsulated form in terms of skin penetration, retention on the skin surface and photo-stability. For the encapsulated form, the UV filters were entrapped inside sol-gel silica glass microcapsules sufficiently small to be transparent when applied to the skin and provide a pleasant skin feeling. FTIR imaging spectroscopy and ATR-FTIR Spectroscopy techniques were used to investigate the penetration of the UV filters into the stratum corneum and their retention overtime on the skin surface. The photo-stability of the sunscreen formulations was evaluated using two criteria: (i) Area Under the curve (AUC) and (ii) SPF values calculated in-vitro following the COLIPA method.

2. Materials and method

2.1. Chemicals

Avobenzone (INCI: Butyl Methoxydibenzoylmethane, Eusolex 9020), Octocrylene (Eusolex OCR), Eusolex® UV-Pearls™ B-O X (INCI: Aqua, Octocrylene, Sorbitol, Butyl Methoxydibenzoylmethane, Silica, PVP) from Merck®; Xanthan gum and Glycerin from Sigma-Aldrich®; Tegosoft TN (C12-15 Alkyl Benzoate) and Abil XL80 (Bis-PEG/PPG-20/5 PEG/PPG-20/5 Dimethicone (and) Methoxy PEG/PPG-25/4 Dimethicone (and) Caprylic/Capric Triglyceride) from Evonik®; Euxyl 9010 (INCI: Phenoxyethanol and Ethylhexylglycerin) from SchÜlke®.

2.2. Morphological evaluation by scanning electron microscopy (SEM)

Morphological evaluations of the encapsulated UV filter were performed using scanning electron microscopy (SEM). The SEM used was a FEI XL30 FEG-SEM equipped with an EVEX EDS. The samples were coated with iridium by a sputter coater (Leica EM ACE600). The SEM pictures were recorded at 5KeV with a working distance of ~15 mm. Low magnification (2500×) and high magnification (6000×) were used.

2.3. Skin samples

The skin samples were obtained from the belly of pig. They were flash frozen with liquid nitrogen and stored at −40 °C wrapped in aluminum foil until the use. Before to start the experiments, the skin samples were defrosted at room temperature for 20 min. Skin pieces 2 × 2 cm or 2 × 7 cm were cut and cleaned to remove dirt and sebum.

2.4. Formulation tested

Free and encapsulated UV filters were incorporated in a cold lotion water-based. F1 represents the formulation without actives; F2 is the formulation containing UV filters (Butyl Methoxydibenzoylmethane and Octocrylene) in free form and the formulation F3 contains encapsulated UV filters (Butyl Methoxydibenzoylmethane and Octocrylene). The detailed composition of those formulations is shown Table 1. The formulation tested was made to obtain sunscreen with moderate SPF. BASF Sunscreen Simulator software was used to evaluate the theoretical performances of the formulations regarding SPF (Herzog and Osterwalder, 2015).

Phase A and phase B are stirred separately. Phase B was addicted to phase A under stirrer for 5 min at 1000 rpm following by 2 min at 200 rpm by Apolytron PT 10-35 (Kinematica). At the end, phase C was added to the formulation. Formulation were stored at 25 °C for 14 h

Table 1
Detailed composition of each formulation tested in this study.

Phase	Ingredient	INCI	F1	F2	F3
A	Water	Water	83.1	71.1	53.1
	Xanthan gum	Xanthan gum	0.9	0.9	0.9
	Glycerin	Glycerin	2	2	2
	UV Pearls	Water, octocrylene, sorbitol, butyl methoxydibenzoylmethane, silica, PVP	–	–	30
B	Tegosoft TN	C12-15 alkyl benzoate	10	10	10
	Abil XL 80	Bis-PEG/PPG-20/5 PEG/PPG-20/5 dimethicone (and) methoxy PEG/PPG-25/4 dimethicone (and) caprylic/capric triglyceride	3	3	3
	Eusolex 9020	Butyl methoxydibenzoylmethane	–	3	–
	Eusolex OCR	Octocrylene	–	9	–
C	Euxyl 9010	Phenoxyethanol and ethylhexylglycerin	1	1	1

before direct stability characterization. A multisampling analytical centrifuge Hettich® Universal 320R D-78532 PRO Scientific Inc. USA was used in two phases to assess the stability of these formulations: 10 min, 3000 rcf, 25 °C and right after 30 min, 5000 rcf, 25 °C.

2.5. Skin treatment

Cleaned skin samples were treated with 2 mg/cm^2 of sunscreen formulations applied topically with 1 min of massage to cover the entire skin surface uniformly and mounted in diffusion cells (PermeGear, Inc. USA) 15 mm jacketed Franz Cell system with 12 mL receptor chamber filled by phosphate buffer solution pH 7.2 (Fluka Analytical). The diffusion cells were connected to heated bath circulators to maintain the temperature constant at 32 °C. The skin samples were maintained in this condition for 2 h for the penetration measurement and during 4 h for the retention measurement on the skin surface.

2.6. Skin penetration measurement

2.6.1. Tape stripping

At the end of the 2 hour treatment, the skin samples were removed from the diffusion cells and the sunscreen remaining on the skin surface was gently removed with three spatula movements before analysis. Tape stripping technique is a well-established method to investigate the skin penetration of topically applied substances inside the stratum corneum (Lademann et al., 2009). This non-invasive procedure (Klang et al., 2012) sequentially removes layers of stratum corneum from ex-vivo or in-vivo skin samples. Commercial adhesive tape (Scotch™) was used. The adhesive tapes were applied onto the skin surface, followed by gentile pressure to guarantee a good contact between the most superficial SC layer and the adhesive tape and progressively removed. The pressure, velocity of removal and the type of tape are factors influencing the amount of Stratum Corneum removed per each strip. To standardize the procedure, the same operator applied with the finger a constant pressure on the tape and the same velocity to remove the tape strips. After every removal the skin samples were scanned by FTIR imaging.

2.6.2. FTIR imaging analysis

All the FTIR images were acquired with a Spotlight 400 Imaging System (Perkin Elmer Instruments, USA) using a MCT (mercury-cadmium-telluride) focal plane array detector. FTIR images were collected in reflective mode with an ATR imaging accessory at a spectral resolution of 4 cm^{-1} in the mid-infrared (MIR) region between 4000 and 850 cm^{-1} with a spatial resolution of 6.25 × 6.25 µm and sample size of 300 × 300 µm. The ATR imaging accessory used a germanium crystal placed directly in contact with the skin samples. The FTIR Imaging System records hyperspectral images that can provide maps showing the co-localization of specific molecular components or spectroscopic parameters. These images are generated with false colors where the red represent highest values and blue lowest values for each parameter investigated. By scanning skin samples after sequential tape strips, an FTIR spectroscopic "mapping" inside the stratum corneum can be obtained. These maps were used to visualize the penetration of the UV filters inside the stratum corneum.

2.7. Retention measurement on the skin surface

2.7.1. ATR-FTIR spectroscopy

The retention of UV filters on the skin surface was investigated by ATR-FTIR spectroscopy (Nicolet 6700-Thermo Scientific) after topical application of the sunscreen formulations at different time points; 30 min, 1 h, 2 h and 4 h. After every time point the surface of skin samples were scanned by ATR-FTIR Spectroscopy. ATR-FTIR spectra were recorded in the mid-IR region range from 400 to 750 cm^{-1} with a spectral resolution of 4 cm^{-1} and 64 scans accumulation.

2.8. Spectroscopic data processing

FTIR spectra and FTIR images presented in this work were processed using GRAMS/AI (Thermo Fisher Scientific) and ISys software from Spectral Dimensions (Olney, MD) respectively. Using these software spectroscopic parameters were defined to investigate and follow specifically the UV filters tested in this study inside the skin samples. In order to have an optimal data interpretation pre-processing technique were used. Its aim is increase the interpretability and accuracy of the data correcting issues associated with spectral data acquisition (Rinnan et al., 2009). All the FTIR spectra were baseline corrected. In previous study, the Amide I and II band shape and position were evaluated and a similarity between the mean spectra of Amide I and II in different deep was found. The contribution to absorbance in the Amide I and Amide II region are essentially constant in relation to the deep (Zhang et al., 2006). All the FTIR spectra were normalized using the Amide I peak (1710–1590 cm^{-1}).

2.9. Photo-stability evaluations

Sunscreen samples were irradiated by Xenon Lamp with QSun Xenon Test Chamber 3100. This system is able to reproduce the damage caused by full-spectrum sunlight, the sample was exposed to irradiance: 0.55 ± 2 W/m^2 with a temperature: 40 ± 1 °C and humidity: 45 ± 1%. Photo-stability of the sunscreen formulations were evaluated by the Area Under the curve (AUC) (Gonzalez et al., 2007). The Area Under the Curve (AUC) for both UVB (290–320 nm) and UVA (320–400 nm) were calculated for each sunscreen on PMMA plate before and after UV exposure. The AUC were calculated following the equation:

$$AUC\ UVR = \int_{290}^{400} A\lambda\ d\lambda$$

$$AUC\ UVB = \frac{1}{2}A320 + \int_{290}^{319} A\lambda\ d\lambda$$

$$AUC\ UVA = \frac{1}{2}A320 + \int_{321}^{400} A\lambda\ d\lambda$$

where A is Absorption and d the wavelength.

To compare the photo-stability for each sunscreen before and after exposure the areas under the curve were compared using Student's t-test ($p < 0{,}05$). The AUCI (Area Under the Curve Index) was calculated following the equation:

$$AUCI = \frac{AUC\ after}{AUC\ before}$$

If the AUCI was ≥0.8 the sunscreen was considered photo-instable.

The ratio between the irradiated and non-irradiated samples curve areas was calculated following the equation:

$$Ratio = \frac{AUC\ after}{AUC\ before} * 100$$

The results were reported in percentage.

The SPF in vitro was calculated with the well-established method by the International Sun Protection Factor Test Method COLIPA (Cosmetics, 2011). Cosmetics Europe (the European Cosmetic Products Trade Association defined equation for the estimation of SPF in vitro:

$$SPF\ in\ vitro = \frac{\int_{\lambda=290\ nm}^{\lambda=400\ nm} E\lambda\ I\lambda\ d\lambda}{\int_{\lambda=290\ nm}^{\lambda=400\ nm} E\lambda\ I\lambda\ 10^{-A0\lambda} d\lambda}$$

where: E λ = Erythema action spectrum (CIE-1987), I λ = Spectral irradiance of the UV Source (SSR for SPF testing), A_0 λ = Mean monochromatic absorbance measurements per plate of the test product layer before UV exposure, d λ = Wavelength step (1 nm).

2.9.1. Spectrophotometric measurements

Substrate and product application were carried out in according to the COLIPA Method (Cosmetics Europe, 2011). 1.3 mg/cm^2 of sunscreens products were spread on roughened PMMA plate (SUNPLATES PMMA plates (5 cm × 5 cm) roughness 4.5 to 5.5 µm Lot. XT 1601-1 by HelioScience® Sun Technology). The formulation was applied as a large number (approximate 12) of small drops (approximate equal volume) over the whole surface of the PMMA plate. After application, the formulation was spread using a fingertip "pre-saturated" with the formulation. Spreading is two phases process: (i) product distribution with quickly movements but without pressure (30 s.), (ii) circulate movements using pressure (30 s.) The samples were left 30 min in the dark 25 °C to facilitate the formation of standard product film. Each formulation was spread onto three PMMA plates and each plate was measured in five different sites to ensure a total area of 5 cm^2.

The absorption curve before and after irradiation was recorded with an UV/Vis/NIR Spectrophotometer equipped with a 150 mm integrating sphere (Lambda 1050 from PerkinElmer). The plates were placed into the spectrophotometer transmittance port facing the light emission source. A 100% transmission reference sample was prepared by spreading 15 µl of Glycerin on the roughened side of the PMMA plate. UV Measurement method: set the scan range from 400 nm to 290 nm, ordinate mode of T%, data Interval 1 nm, bandpass (PMT fixed) of 2 nm, Integration time of 0.2 nm. All obtained transmittance values were converted to absorbance according with the equation (Cosmetics Europe, 2011):

$$A\lambda = -\log(T\lambda)$$

where A λ = Mean monochromatic absorbance measurements and T λ = Fraction of incident transmitted by the sunscreen film.

3. Results and discussion

3.1. Morphological evaluation of encapsulated UV filters

The encapsulated UV filter evaluated in this study used micro-encapsulation technology that entraps organic chemicals in sol-gel silica glass. This process produces aqueous dispersion of capsules with approx. 37% (w/w) of UV absorber. Those capsules were prepared by polycondensation reaction at room temperature. This type of low temperature glass synthesis enables substances such as organic UV filters to be encapsulated within the glass by adding them to a reaction mixture. Approximately 80% of the capsule's weight is made up of the UV absorber. Fig. 1 shows scanning electron microscopy (SEM) images of obtained sol-gel silica-shell. The capsules were formed as sphere with calculated average diameters of ~1–2 µm. The capsules were sufficiently small to be transparent when applied to the skin and provide a pleasant skin feeling.

3.2. IR marker used to follow the UV filters

All the formulations were shown to be stable. Formulations F1, F2 and F3 were scanned by FTIR Spectroscopy. The resulting FTIR spectra and second-derivative spectra of the formulation F1, F2 and F3 were used to define the most relevant IR marker to investigate the UV filters used in this study. Average spectra for each formulation F1, F2 and F3 were calculated from several IR spectra recorded on each formulation and the second-derivative spectra were obtained from these average spectra. In Fig. 2, significant differences were observed between these 3 FTIR spectra, the most prominent being the band at 1231 cm^{-1} (Fig. 2b). The band at wavenumber 1231 cm^{-1} can be observed in the spectra recorded on the formulation F2 and F3 but this contribution is absent in the spectrum recorded on the based formulation F1 without the UV filters. Deepest investigations were made in order to validate the IR peak at 1231 cm^{-1} as an IR marker of the UV filters. Second derivative spectra of formulation F1, F2 and F3 were obtained (Fig. 2c) and clearly the IR contribution at 1231 cm^{-1} was observed only in the formulation containing the UV filters; F2 and F3.

The FTIR spectra recorded on Avobenzone and Octocrylene (raw material) are presented in Fig. 3. The IR contribution detected around wavenumber 1231 cm^{-1} in the formulations F2 and F3 is consistent with the IR band observed around 1226 cm^{-1} in the spectrum of the Avobenzone (Fig. 3b) validating the assignment of the band at 1231 cm^{-1} to the avobenzone contribution. The shift from 1226 cm^{-1} to 1231 cm^{-1} can be explained by the modification that the Avobenzone powder underwent when it was added into the formulation. No Octocrylene contribution was observed in this area (Fig. 3b, C). All together, these data shown the Avobenzone content can be monitored by the IR band at 1231 cm^{-1}. Avobenzone is the most important organic UVA absorber that has been globally approved, Octocrylene is used mostly to stabilized and solubilized the Avobenzone implementing the level of primary photoprotection (Lionetti and Rigano, 2017; Afonso et al., 2014) (Wang et al., 2010). In the presented study, Avobenzone was considered as the principal UV filter in order to evaluate the penetration and the retention of organic UV filter into the stratum corneum.

3.3. Deposition and penetration of the UV filter

To investigate the impact of the formulation on the penetration behavior of the UV filters inside the stratum corneum, 3 different sunscreen formulations (F1, F2 and F3) were applied topically on skin samples. Skin from many mammalian species, including pig and humans, can be used to evaluate the penetration of cosmetic products into the skin as the permeability properties are maintained after excision (Lademann et al., 2009). Indeed, the integrity of the stratum corneum, the main component for the skin barrier function, is not altered. Skin samples were scanned by ATR-FTIR Imaging Spectroscopy in association with a tape stripping procedure to provide a penetration profile of exogenous UV filters into the stratum corneum. Four skin samples were analyzed and compared: skin treated with formulation F1, F2 and F3 were compared with untreated skin. For each sample FTIR images were scanned before (control), after topical treatment (deposition) and after the tape strip were removed. The FTIR images were concatenated to produce the FTIR Images shown in Fig. 4. These FTIR images were generated to follow specifically the UV filters in the skin samples by using the wavenumber 1231 cm^{-1} to Amide I intensity ratio. This ratio allows to visualize specifically the Avobenzone inside the skin samples and in consequence was used to compare the penetration of this active in function of the different sunscreen formulations.

As expected the Avobenzone was not detected in all the skin samples before treatment, in the untreated skin and in the sample treated with formulation F1. High deposition of UV filter on the skin surface was recorded on skin samples treated with formulation F2 and F3. As discussed previously, sunscreen should have a high affinity for stratum corneum to stay and adhere on the superficial layer of the skin to create a protective and stable film. The high active concentration observed on the skin surfaces after the treatment (deposition) demonstrated the formulation F2 and F3 have created a uniform protective film on the skin surface. The FTIR Imaging technique coupled with a tape stripping procedure allows to visualize and compare the UV filter penetration into the stratum corneum related to a specific sunscreen formulation. In this work we detected, a different penetration behavior for the Avobenzone between the traditional sunscreen formulation and the sunscreen formulation based on encapsulation technology. With the regular formulation, the UV filters presented as expected a high concentration on the skin surface but also a significant concentration deep inside the stratum corneum indicating the Avobenzone under "free" formulation did not remain on the skin surface but penetrated deep inside the skin. Indeed, the UV filters were detected up to the layer 6 under free formulation after just one single topical application. On the other hand, the same UV filter combined with encapsulation technology

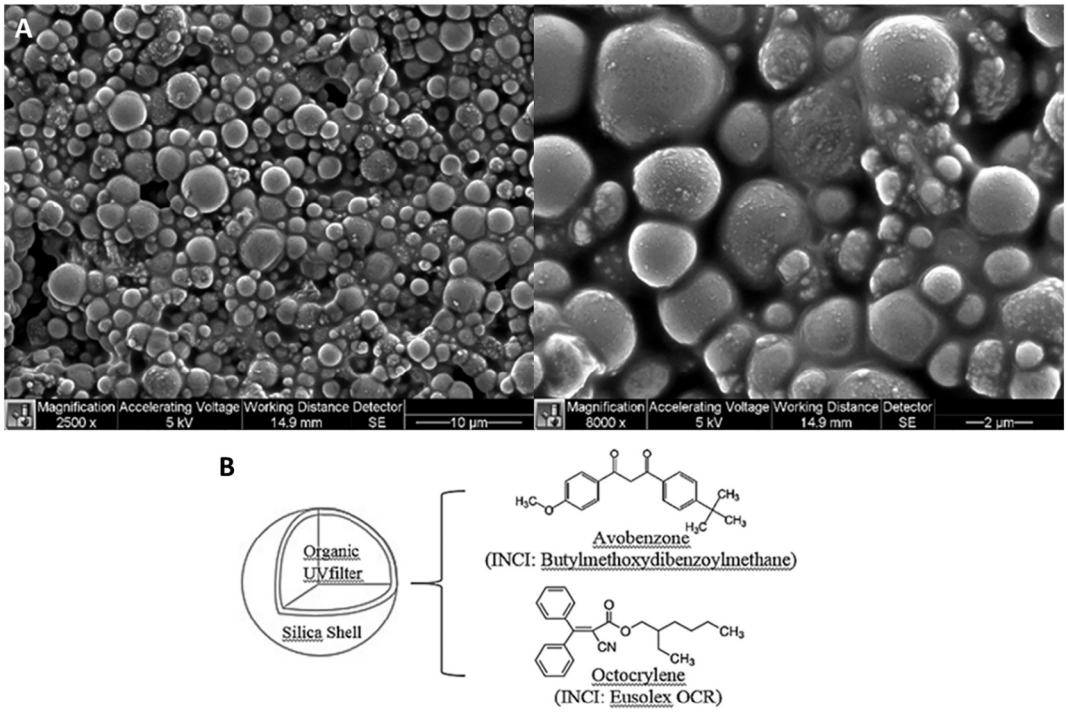

Fig. 1. a) SEM pictures recorded on Eusolex UVPearls (Merck). The SEM pictures present the capsules loaded with Avobenzone and octocrylene at low magnification (2500× on the left) and high resolution (6000× on the right) b) illustration of Avobenzone/Octocrylene silica shell capsules.

were observed on the skin surface and almost no penetration was detected inside the stratum corneum. Indeed, the encapsulated avobenzone was not detected after the layer 1 clearly indicating that the encapsulation technology allowed to keep the UV filters at the surface of the skin where they will the most efficiently exert their purpose.

The current results are in accordance with earlier investigation (Scalia et al., 2011) which studied the effect of encapsulation technology on the penetration of Ethylhexyl Methoxycinnamate (EHMC) and Butyl Methoxydibenzoylmethane (Avobenzone) in human skin. The study demonstrated that sunscreen loaded in lipid microparticles

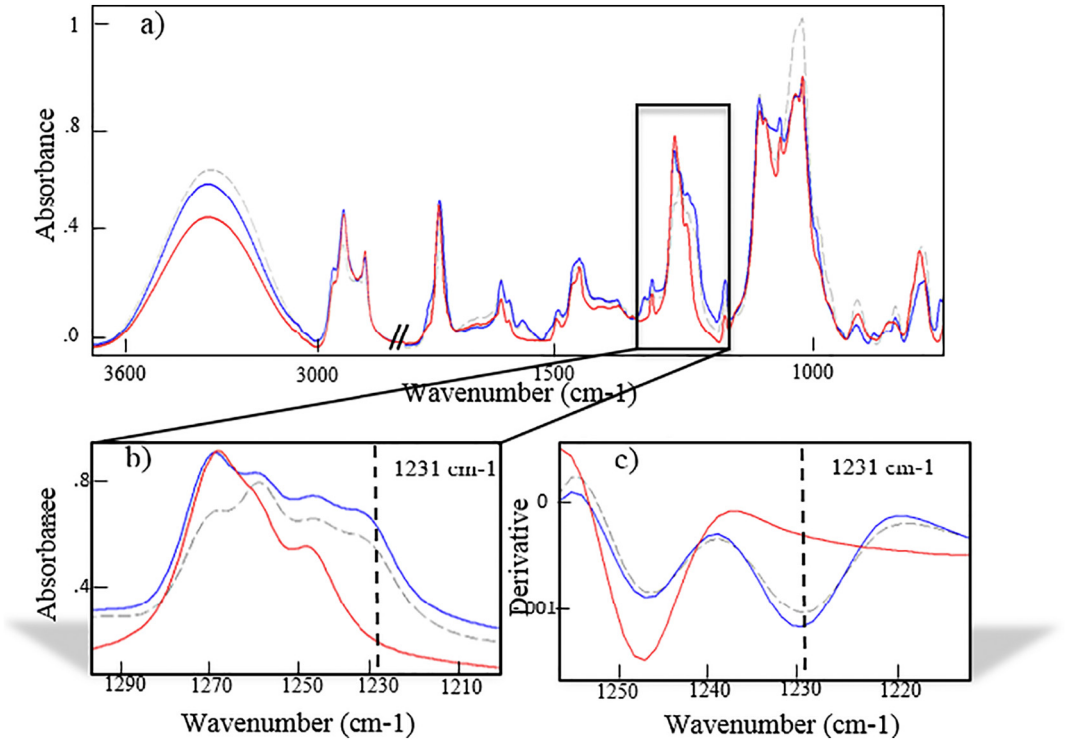

Fig. 2. a) mean FTIR spectra between 3600 and 850 cm^{-1} region b) enlargement in the 1290–1210 cm^{-1} region and c) second derivative spectra recorded on formulation F1 (red line), F2 (dashed grey line) and F3 (solid blue line). (For interpretation of the references to color in this figure legend, the reader is referred to the web version of this article.)

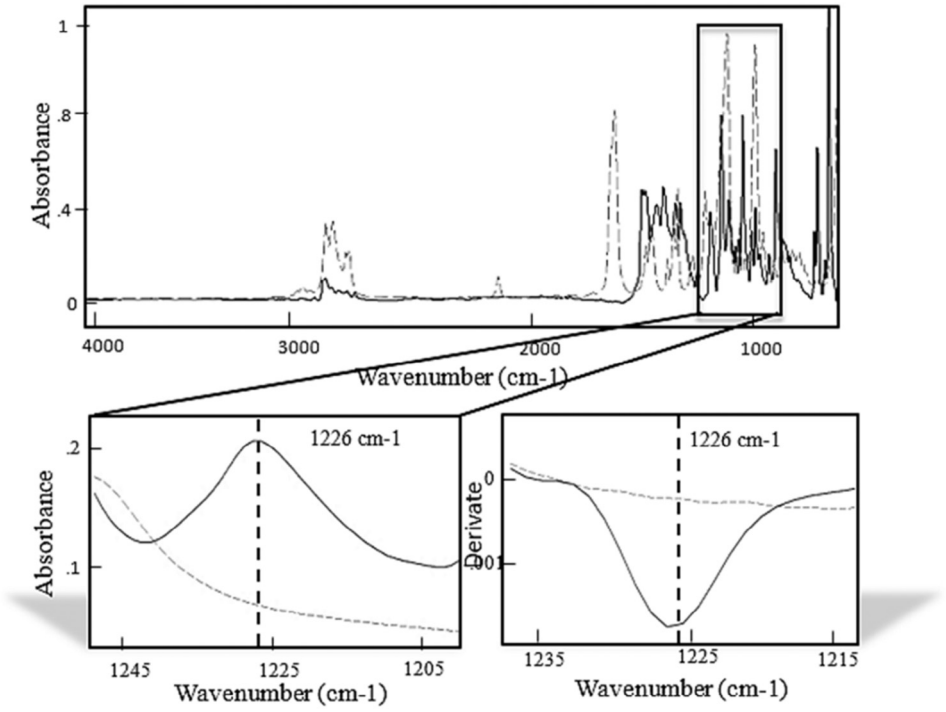

Fig. 3. a) Mean FTIR spectra recorded between 4000 and 850 cm^{-1}, b) enlargement in the 1280–1200 cm^{-1} region and c) second derivative of Avobenzone powder (solid line) and Octocrylene (dashed grey line).

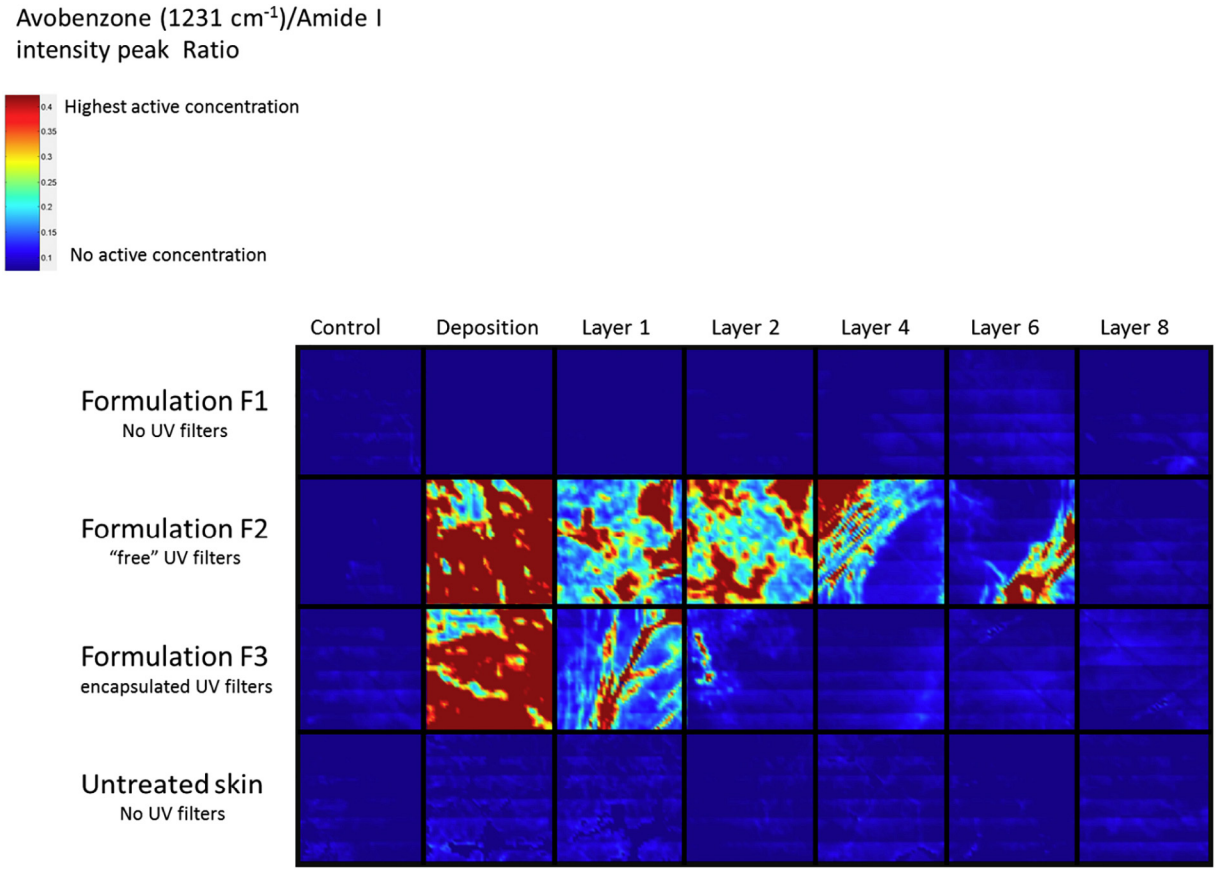

Fig. 4. FTIR images generated by calculating the intensity peak ratio between 1231 cm^{-1} (Avobenzone) and the Amide I. These FTIR Images allow to visualize and compare the avobenzone penetration inside the stratum corneum for different skin samples: skin samples treated with formulation F1, F2 and F3 compared to untreated skin. For each sample the FTIR images were scanned before (control), after topical application on the sunscreen formulation and after 8 sequential tape strips.

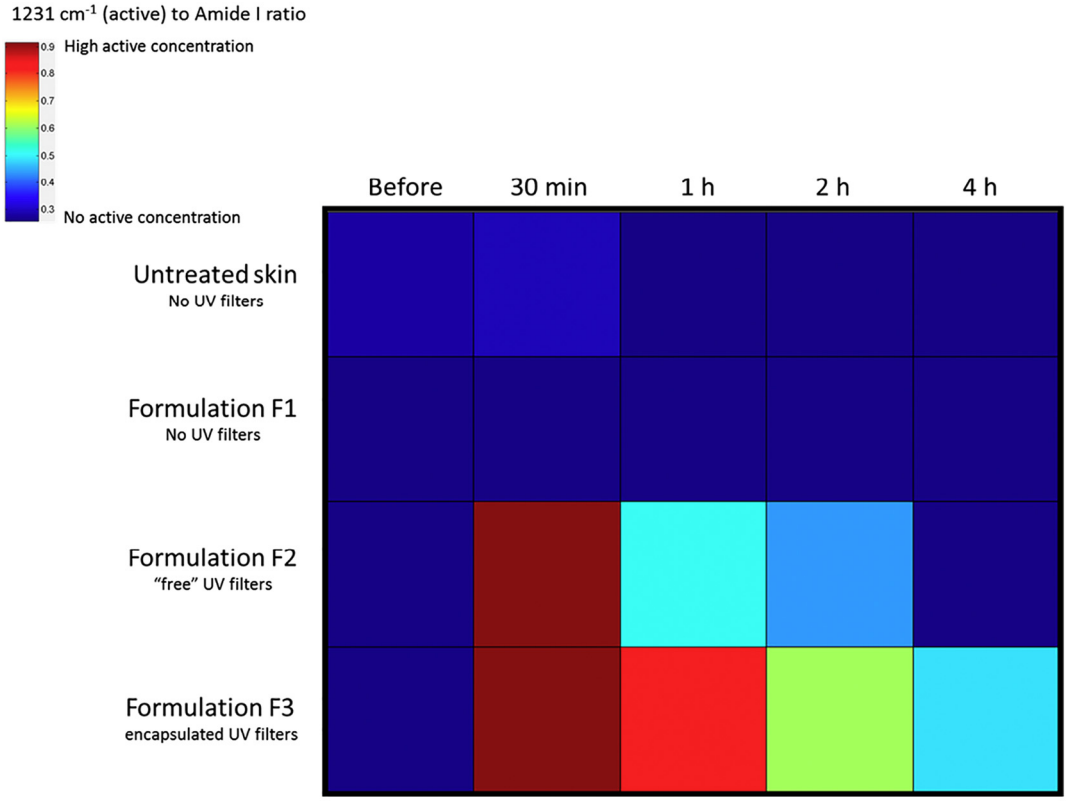

Sample	Time				
	Before	30 min	1 h	2 h	4h
Untreated	0.28	0.29	0.25	0.26	0.19
Formulation F1	0.26	0.21	0.26	0.20	0.21
Formulation F2	0.23	1.48	0.51	0.44	0.24
Formulation F3	0.18	1.27	0.83	0.61	0.48

Fig. 5. FTIR images were generated by calculating the 1231 cm^{-1} to Amid I intensity peak ratio from skin samples treated with formulation F1, F2 and F3 before (control), after (deposition) up to layer 8, compared to untreated skin.

penetrated less depth into the stratum corneum compared to the UV filters "free". The main fraction of the sunscreen which penetrated the skin was localized only in the upper layers of the skin. More recently (Puglia et al., 2014) another group evaluated the nanostructured lipid carriers (NLC) to optimize the topical application of organic UV filters. In agreement with our study, this previous report showed that this different NLC encapsulation technology limits skin penetration of UV filters that remained primarily on the surface of the skin.

3.4. Retention overtime

To validate the previous data and assess their impacts on the efficacy of these different sunscreen formulation technologies we analyzed the retention of the Avobenzone overtime on the skin surface. This test provided relevant data concerning the UV filters incorporated in the formulations in term of deposition on the skin surface and how long these UV filters stay on the surface in function of the sunscreen technologies used to elaborate the formulations. The FTIR images presented in Fig. 5 were generated using the same intensity ratio between the Avobenzone (1231 cm^{-1} region) and the Amide I. These FTIR images confirmed the previous data concerning the UV filter concentration on the skin surface. The FTIR images were generated with false color. Redder was the image, higher was the Avobenzone concentration on the skin surface. Skin samples treated with formulation F2 and F3 presented the highest concentration of UV filter after 30 min confirming the ability of these formulations to create a protective film on the superficial areas of the skin. This uniform coating provided the skin protection against the UV radiation. The presence of this coating overtime and as well as its stability will determine the efficacy of the sunscreen formulation. Sample treated with formulation F2 showed a significantly lower concentration of UV filter on the skin surface after exposure for an hour. This tendency is confirmed and amplified after 2 h and even more after 4 h. Indeed, after 4 h the IR ratio calculated on the sample was similar to the one recorded before treatment indicating that after 4 h no more UV filter was present on the skin which was treated with the sunscreen formulation F2. These data provided information regarding the inclination for the organic UV filters to go across the stratum corneum especially in regular sunscreen formulation where the UV filters are "free". To limit this penetration and improve the efficiency of the sunscreen, encapsulation technology is a relevant option to formulate UV filters in sunscreen products. Indeed, samples treated with formulation F3 based on encapsulation technology presented a similar UV filter concentration level than the one observed in the skin treated with the formulation F2 after 30 min. In contrast, after 2 h and 4 h, a significantly higher amount of Avobenzone was still detectable on the skin surface after topical application of the formulation

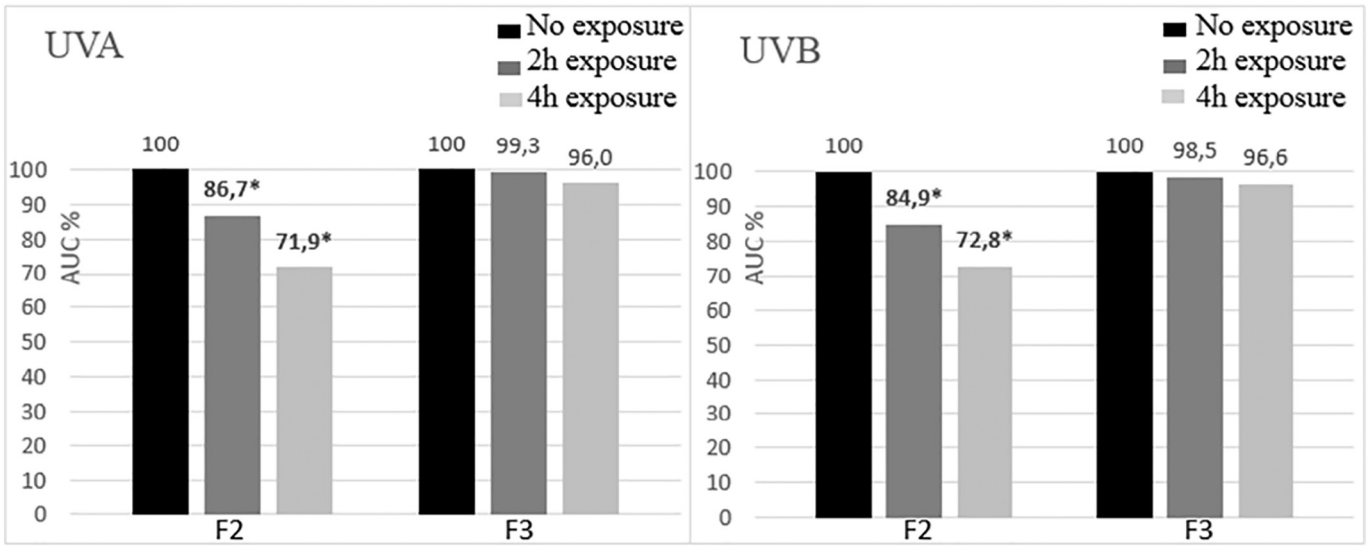

Fig. 6. Area under the absorption curve % (AUC) before, after 2 h and 4 h of UV exposure recorded on formulation F2 (free) and F3 (encapsulated) for the UVA (320–400 nm) and the UVB (290–320 nm). The areas were compared using Student's *t*-test ($p < 0,05$), The results statistically different ($p < 0,05$) were marked with *.

F3 compared with the formulation F2 highlighting the ability of the encapsulation technology to reduce the penetration of the UV filter in the skin and in consequence to improve the efficacy of the sunscreen product.

3.5. Photo-stability evaluation after exposure

Photo-stability of sunscreens is a key parameter that must be taken into consideration during their development and to assess their performance especially when they incorporate organic UV filters. Organic UV filters were designed and used to efficiently absorb the UV radiation during a given time period. This absorption can induce photochemical reactions in these molecules which result in some degradation of these UV filters and in consequence decrease the efficiency of the sunscreen products (Nash and Tanner, 2014; Kockler et al., 2012). To strengthen the previous data and to confirm the benefit of the encapsulation technology in term of sunscreen efficacy, we analyzed and compared the photo-stability of these sunscreen formulations. The first parameter used to evaluate the photo-stability was the area under the curves (AUC). The AUC calculated versus wavelength (290–320 nm for UVB and 320–400 nm for UVA) before and after irradiation are presented in Fig. 6.

The sunscreen protection provided by the formulation F2 decreased significantly overtime under UV exposure. Formulation F2 designed with “free” UV filters showed a reduction of 13% in the UVA protection and 15% in the UVB protection abilities after two hours of UV exposure. This degradation was confirmed and amplified after 4 h of UV exposure. Indeed, the formulation F2 showed a reduction of 28% in the UVA protection and 27% in the UVB protection after 4 h of UV exposure. The AUCI for formulation F2 after 2 h of exposure was 0.86 and 0.72 after 4 h. F2 presented unstable behaviors when exposed to UV radiation. Formulation F3 did not present a statistically significant reduction in their UVB or UVA absorption after irradiation. The AUCI value for F3 after 2 h of exposure was 0.99 and 0.96 after 4 h indicating a photostable behavior for F3. Data have shown the encapsulation technology associated with a combination Avobenzone/Octocrylene could prevent efficiently the photo-degradation of the sunscreen products formulated with organic UV filters. These data can be compared with a previous study (Yang et al., 2008) which investigated the influence of hydroxypropyl-beta-cyclodextrin (HPCD) complexation on the photodegradation of Avobenzone. The complexation was shown to significantly reduce the photodegradation of Avobenzone after UV irradiation for 16, 40 and 80 min.

The effect of the temperature on the PMMA plate could create some interference in the absorbance curve determination. In order to eliminate the interference of the temperature after 2 h and 4 h of UV exposure, PMMA plates without formulation were studied in the same testing condition but without UV exposure. The analysis shown thermal stability of the PMMA plate (data not presented).

The second parameter used to evaluate the photo-stability of formulation tested is the SPF (Sun Protection Factor). Absorbance spectra for formulations F2 and F3 as well as percent variance of SPF values before and after 2, 4 h of UV exposure are shown in Fig. 7. By evaluating the spectra of sunscreen formulation F2 before and after exposure, an absorption decreases in UVA and UVB region was observed. Formulation F2, with free form of UV filters, exhibited a decrease of 31% in SPF value after 2 h of exposure and 50% after 4 h of UV exposure. A significant reduction in SPF values can be associated with a decrease in photoprotection effectiveness of the sunscreen formulation. An insignificant reduction in SPF values were detected for formulation F3 after 2 and 4 h. These results confirm that encapsulation technology can maintain “the in-vitro SPF values of UV filters” and consequently be a good strategy to improve the photo-stability of organic UV filters.

4. Conclusions

Extended exposure to ultraviolet radiation plays a prevalent role in skin damages like photo-carcinogenesis or photo-aging. Sunscreens are currently leading products to protect our skin and avoid these alterations. With the continuous increase in air pollution levels and global warming, sunscreens will become even more essential products in our day-to-day life. While no regulations are yet established in terms of sunscreen skin penetration and stability, a growing customer safety concern should be taken seriously into consideration when designing future sunscreen products. To respond to these new international market needs, companies must develop new UV filters and innovative technologies to provide safe, more efficient and flexible sunscreen products not only protecting against skin damages, but also providing a pleasant application experience and visual finish for cosmetic perspective. In the present study, we show that FTIR spectroscopy and FTIR imaging techniques are efficient methods to investigate and visualize several essential parameters of new sunscreen formulations,

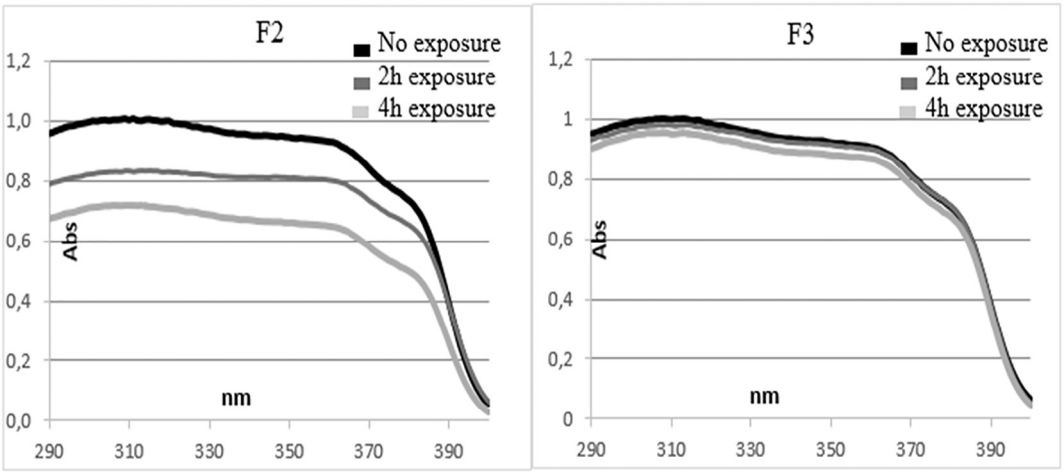

Sample	Variation % SPF in vitro	
	2 h exposure	4 h exposure
F2	31.5	50.7
F3	3.9	8.4

Fig. 7. UV absorbance spectra of formulation F2 and F3 and percent variance of SPF values calculated in-vitro before and after 2 and 4 h of UV exposure.

such as their penetration profile inside the skin and their retention on the skin surface. Notably, we show that sunscreens based on encapsulation technology can reduce the penetration of the organic UV filters inside the skin improving thereby their overall safety. Performance is also increased by this process knowing that encapsulated organic UV filters showed a significantly extended photostability. In conclusion, this work highlights the potential of innovative strategies such as micro-encapsulation technology, to become a relevant plan of action to produce superiorly efficacious organic UV filters-based sunscreen products with limited toxicological risks.

References

Afonso, S., Horita, H., Sousa e Silva, J.P., Almeida, M.H., Lobao, P.C., Costa, P.A., Miranda, M.S., Joaquim, C.G., Esteves, Silvia, Sousa Lobo, J.M., 2014. Photodegradation of avobenzone: Stabilization effect of antioxidants. J. Photochem. Photobiol. B 140, 36–40.

Benita, S., 2005. Microencapsulation: methods and industrial applications. In: Drugs and the Pharmaceutical Sciences, 2nd edn. CRS Press, New York, pp. 79–86.

Brash, D.E., Rudolph, J.A., Simon, J.A., Lin, A., McKenna, G.J., Baden, H.P., Halperin, Pontén, J., 1991. A role for sunlight in skin cancer: UV-induced p53 mutations in squamous cell carcinoma. Proc. Natl. Acad. Sci. 88 (10), 124–128.

Cabrera, C.G., Madrid, J.F.P., Arteaga, J.D.P., Alejandro, M.E., 2014. Characterization of encapsulation process of Avobenzone in solid lipid microparticle using a factorial design and its effect on photostability. J. Appl. Pharm. Sci. 4 (12), 35–43.

Cantrell, A., JMcGarvey, D., 2001. Photochemical studies of 4-tert-butyl-40methoxydibenzoylmethane (BM-DBM). J. Photochem. Photobiol. B Biol. 64 (2–3), 117–122.

Cosmetics Europe In vitro UV Protection Method Task Force, 2011. In vitro method for the determination of UVA protection factor and critical wavelength values of sunscreen products. Guardline 1–28.

Damiani, E., Astolfi, P., Giesinger, J., Ehlis, T., Herzog, B., Greci, L., Baschong, W., 2010. Assessment of the photo-degradation of UV-filters and radical-induced peroxidation in cosmetic sunscreen formulations. Free Radic. Res. 44, 304–312.

Gonzalez, H., 2010. Percutaneous absorption with emphasis on sunscreens. Photochem. Photobiol. Sci. 9, 482–488.

Gonzalez, H., Farbrot, A., Larkö, O., Wennberg, A.-M., 2006. Percutaneous absorption of the sunscreen benzophenone-3 after repeated wholebody applications, with and without ultraviolet irradiation. Br. J. Dermatol. 154, 337–340.

Gonzalez, H., Tarras-Wahlberg, N., Strömdahl, B., Juzeniene, A., Moan, J., Larkö, O., Rosen, A., Wennberg, A.-M., 2007. Photostability of commercial sunscreens upon sun exposure and irradiation by ultraviolet lamps. BMC Dermatol. 7 (1), 1–9.

Gonzenbach, H., Hill, T.J., Truscott, T.G., 1992. The triplet energy levels of UVA and UVB sunscreen. J. Photochem. Photobiol. B 377–379.

Halliday, G.B.S., 2014. An unexpected role: UVA induced release of nitric oxide from skin may have unexpected health benefits. J. Int. Dermatol. 134, 1791–1794.

Hayden, C.G., Cross, S.E., Anderson, C., Saunders, N.A., Roberts, M.S., 2005. Sunscreen penetration of human skin and related keratinocyte toxicity after topical application. Skin Pharmacol. Physiol. 18, 170–174.

Herzog, B., Osterwalder, U., 2015. Simulation of sunscreen performance. Pure Appl. Chem. 87, 937–951.

Holick, M.F., 2004. Sunlight and vitamin D for bone health and prevention of autoimmune diseases, cancers, and cardiovascular disease. Am. Soc. Clin. Nutr. 80 (6), 1678S–1688S.

IARC, 2012. IARC Monographs on evaluation of carcinogenic risks to humans, 100D. In: Radiation.

Janjua, N.R., Kongshoj, B., Andersson, A.M., Wulf, H.C., 2008. Sunscreens in human plasma and urine after repeated whole-body topical application. J. Eur. Acad. Dermatol. Venereol. 22, 456–461.

Jiang, R., Roberts, M.S., Prankerd, R.J., Benson, H.A.E., 1997. Percutaneous absorption of sunscreen agents from liquid paraffin: self-association of octyl salicylate and effects on skin flux. J. Pharm. Sci. 86, 791–796.

Jyothi, V.N., Muthu Prasanna, P., Narayan Sakarkar, S., Surya Prabha, K., Ramaiah, S., Srawan, G.Y., 2010. Microencapsulation techniques, factors influencing encapsulation efficiency. J. Microencapsul. 27 (3), 187–197.

Kaur, L.P., Sharma, S., 2013. Microencapsulation: A new era in noval drug delivery. Int. J. Pharm. Bio-Sci. 2 (2), 456–468.

Klang, V., Schwarzb, J.C., Lenobela, B., Nadja, M., Auböckc, J., Wolztd, M., Valenta, C., 2012. In vitro vs. in vivo tape stripping: validation of the porcine ear model and penetration assessment of novel stearate smultions. Eur. J. Pharm. Biopharm. 80 (3), 604–614.

Kockler, J., Oelgemöller, M., Robertson, S., Glass, B.D., 2012. Photostability of sunscreen. J. Photochem. Photobiol. C 13 (1), 91–110.

Lademann, J., Jacobia, U., Surberb, C., Weigmanna, H.-J., Fluhrc, J.W., 2009. The tape stripping procedure – evaluation of some critical parameters. Eur. J. Pharm. Biopharm. 72 (2), 317–323.

Lionetti, N., Rigano, L., 2017. The new sunscreens among formulation strategy, stability issues, changing norms. Saf. Efficacy Eval. Cosmet. 4 (2), 1–11.

Lu, Z.B., 1999. A method for the preparation of polymeric nanocapsules without stabilizer. J. Control. Release 61, 107–112.

Mancebo, S.E., Judy, Y.H., Wang, S.Q., 2014. Sunscreens: a review of health benefits, regulations, and controversies. Photo-Dermatology 32 (3), 255–456.

Motley, R.J., Reynolds, A.J., 1989. Photocontact dermatitis due to isopropyl and butyl methoxy dibensoylmethanes (eusolex 8020 and Persol 1789). Contact Dermatitis 21, 109–110.

Nash, L.F., Tanner, P.R., 2014. Relevance of UV filter/sunscreen product Photostability to human safety. Photodermatol. Photoimmunol. Photomed. 88–95.

Puglia, C., Damiani, E., Offerta, A., Rizza, L., Tirendi, G.G., Tarico, M.S., Curreri, S., Bonina, F., Perrotta, R.E., 2014. Evaluation of nanostructured lipid carriers (NLC) and nanoemulsions as carriers for UV-filters: characterization, in vitro penetration and photostability studies. Eur. J. Pharm. Sci. 23 (51), 211–217.

Rinnan, A., Van Den Berg, F., Engelsen, S.B., 2009. Review of the most common pre-processing techniques for near-infrared spectra. TrAC 28 (10), 1201–1222.
Scalia, S., Mezzena, M., Ramaccini, D., 2011. Encapsulation of the UV filters ethylhexyl methoxycinnamate and butyl methoxydibenzoylmethane in lipid microparticles: effect on in vivo human skin permeation. Pharmacol. Physiol. 24 (4), 182–189.
Schauder, S., Ippen, H., 1986. Photoallergic and allergic contact dermatitis from dibenzoylmethanes. Photo-Dermatology 3, 140–147.
Schlump, M., Kypke, K., Wittassek, M., Angerer, J., Mascher, H., Mascher, D., Vokt, C., Birchler, M., 2010. Exposure patterns of UV-filters, fragrances, parabens, phthalates,organochlor pesticides, PBDEs, and PCBs in human milk: correlation of UV-filters with use of cosmetics. Chemosphere 81, 1171–1183.
Schwack, W., Rudolph, T., 1995. Photochemistry of dibenzoyl methane UVA filters. J. Photochem. Photobiol. B 229–234.
Setlow, R.B., 1966. Cyclobutane-type pyrimidine dimers in polynucleotides. Science 153 (3734), 379–386.
Shaath, N.A., 2010. Ultraviolet filters. Photochem. Photobiol. Sci. 9, 464–469.
Vallejo, J.J., Mesa, M., Gallardo, C., 2011. Evaluation of the avobenzone photostability in solvents used in cosmetic formulation. Vitae 18 (1), 63–71.
Wang, Q.S., Balagula, Y., Osterwalder, U., 2010. Photoprotection: a review of the current and future technologies. Dermatol. Ther. 23, 31–47.
Yang, J., Wiley, C.J., Godwin, D.A., Felton, L.A., 2008. Influence of hydroxypropyl-beta-cyclodextrin on transdermal penetration and photostability of avobenzone. Eur. J. Pharm. Biopharm. 69 (2), 605–612.
Zhang, G., Moore, D.J., Mendelsohn, R., Flach, C.L., 2006. Vibrational microspectroscopy and imaging of molecular composition and structure during human Corneocyte maturation. J. Clin. Investig. Dermatol. 126, 1088–1094.